minerals present in the ore, as references for the infrared studies, gave the semi-quantitative phase composition of the 20 samples.

Dódony (1986) described the green clay mineral as a hydromica with 1M structure (rarely having two- and three-layer polytypes, too). Applying one-dimensional electron-density calculations to determine the chemical composition of the mineral, he gave the formula: $K_{0.725}(Al_{1.275}Mg_{0.725})\ (Si_4O_{10})(OH)_4$ and thus called the mineral alumino-celadonite.

Based on the XPD studies of a mixed sample, B. A. Sakharov used the term "1M celadonite-type Fe-mica" (determined on the base of a reflection at 1.504 Å) for the green phyllosilicate and found that it may contain up to 20% smectitic layers (Varentsov et al., 1988).

Tóth (1990), discussing all the results obtained on the phyllosilicate in a second research report of Grasselly et al. (1990), presented three chemical analyses (all performed in 1989) of celadonite-rich samples (sample #187, #188 and #188a, with the first one being an "average sample" originating from materials collected at different spots of the mine). However, the mismatch between the given chemical data and the supposed dioctahedral mica stucture was not discussed.

A crucial point in the understanding of the ore genesis can be hidden in the 10-Å phyllosilicate of the Úrkút manganese carbonate ore. If it is a primary precipitate (see e.g. Kaeding et al., 1983) and not a product of diagenetic transformation (Varentsov et al., 1988), it can provide a decisive argument for volcanic contribution in the ore genesis. For this reason, we tried to obtain high-quality mineralogical data on the green layer silicate, which became possible only after an appropriate separation procedure was designed for the given mineral assemblage (Mizák et al., 2000; Weiszburg et al., 2004).

Geological setting and general ideas on the ore formation

The Úrkút Manganese Ore Formation, embedded in a pyritic black shale sequence, is a local facies in the Bakony Mountains, Transdanubian Central Range zone (TCR), Hungary (Fig. 1), confined to an area not larger

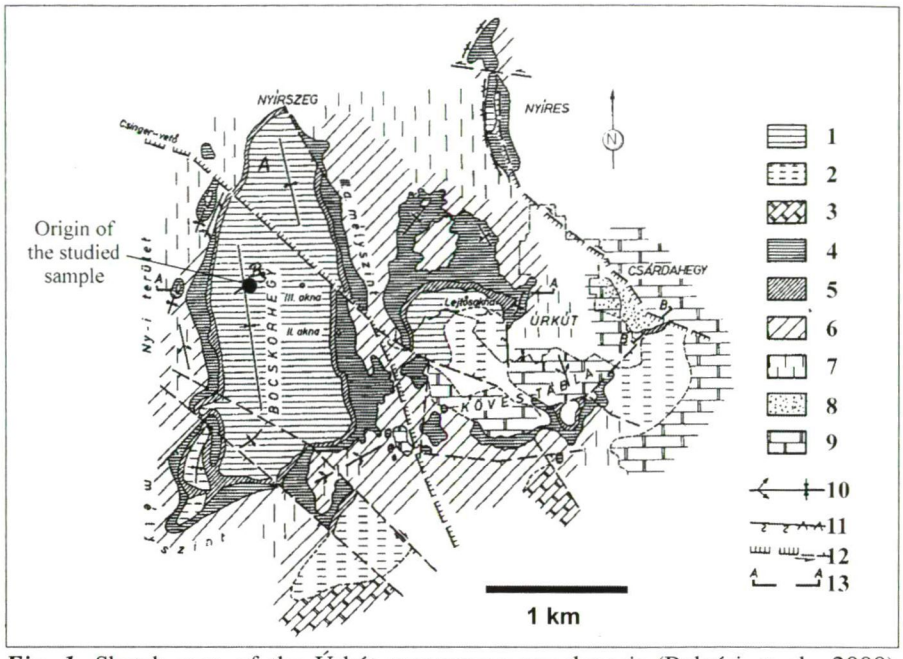

Fig. 1. Sketch map of the Úrkút manganese ore deposit (Polgári et al., 2000). Legend: 1: carbonate ore sequence, complete. 2: carbonate ore sequence, incomplete. 3: hiatus (limestone facies in the Upper Liassic). 4: oxidised manganese ore. 5: transitional zone of carbonate and oxidised ores. 6: redeposited Mn-ore sequence. 7: abraded areas. 8: ferruginous Mn-ore (oxide) of Csárdahegy. 9: underlying rocks. 10: anticline, syncline. 11: flexure, reverse fault. 12: fault, horizontal displacement. 13: profile direction.

than 10 km^2 today. The black shale series is of Early Toarcian age (Falciferum Zone, Géczy in Jenkyns, 1988), and is considered as a product of the Toarcian Oceanic Anoxic Event (Jenkyns, 1988; Jenkyns et al., 1991). Its maximum thickness is about 40 m.

At the time of the black shale formation, the TCR was part of the southern margin of the rifting Tethys Ocean and, as a result of the Sinemurian-Pliensbachian tectonic disintegration, was characterised by dissected and uneven bottom topography, i.e. submarine horsts and basins (Vörös and Galácz, 1998). The black shale sequence was formed in an intrashelf basin of restricted circulation. The depth of the basin is estimated to be around 600 m (Vörös, 1986; Lantos et al., 2003).

The manganese occurs both in carbonate and oxide phases in the ore, with part of the oxide being a secondary product. The manganese carbonate ore forms two horizons in the black shale: the so-called "Main Ore Bed" and "Bed No. II", with maximum thicknesses of 10–12 m and 4 m, respectively (see idealised profile, Fig. 2). The two ore horizons are separated by a dark grey

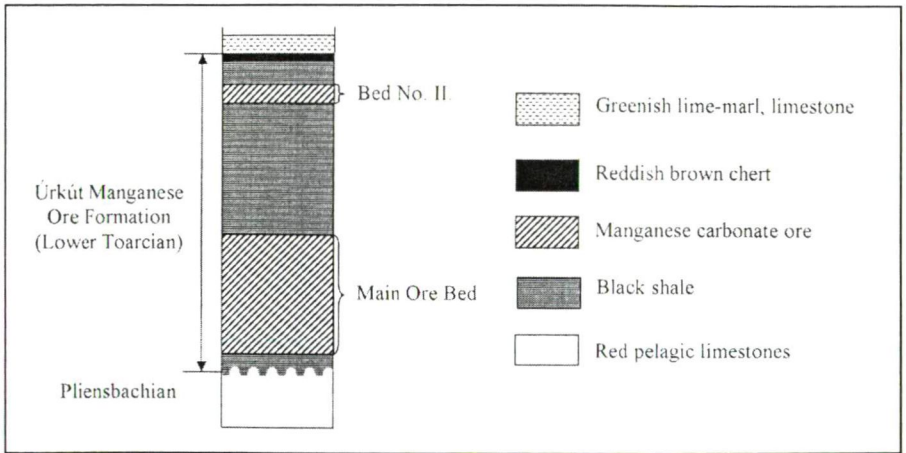

Fig. 2. Schematic profile of the Úrkút manganese carbonate ore (after Polgári et al., 2000).

radiolarian marl ("black shale"). The manganese ore sequence is covered by a brown chert bed of 0.2–0.3 m thickness.

The manganese carbonate ore is banded: green, grey and brown bands of a few centimeters' thickness alternate (Fig. 3). At a higher resolution, the bands are built up of mm-scale light-coloured carbonate-rich and fossiliferous laminae and dark clay-rich laminae, the proportion of dark and light laminae being approximately 9:1 (Lantos et al., 2003). The dark laminae are built up predominantly of the 10-Å green phyllosilicate, rhodochrosite, goethite and other phyllosilicates e.g. smectites (mainly nontronite) while the light laminae are dominated by rhodochrosite and the 10-Å phyllosilicate (Lantos et al., 2003). Based on both sedimentological and mineralogical observations, Lantos et al. (2003) suggest that the material of the whitish laminae was originally deposited on the slopes of a neighbouring undersea high and was later redeposited in the Úrkút basin, while the darker, clay-rich bands deposited in the deepest part of the basin, under suboxic conditions.

The origin of Mn and Fe in these sediments is still debated, both terrigeneous (Szabó-Drubina, 1957, 1959) and volcanogenic-hydrothermal sources have been implied (Szabó-Drubina, 1961; Szabó et al., 1981; Kaeding et al., 1983; Varentsov et al., 1988; Polgári et al., 2000; Polgári, 2001; Lantos et al., 2003). The uncertainties rise from the fact that only indirect evidences exist for volcanism during the Early Toarcian in the TCR (Árgyelán and Császár, 1998). Szabó-Drubina (1957, 1959), based partly on heavy mineral studies, suggested that distant basic igneous and metamorphic rocks, undergoing subaeral erosion could be the source of metals. Manganese and iron were transported into the basin in solution and the Mn- and Fe-bearing minerals were formed by precipitation. Kaeding et al. (1983), considering the different redox potentials of manganese and iron, argued that these elements would have been spatially separated in case they were of terrigeneous origin. They implied that volcanogenic CO_2-rich waters could mobilise these ions from basic lavas and tuffs of the ocean floor in quantities large enough for the ore formation. They interpreted the whole mineral assemblage of the ore as a chemical precipitate. Varentsov et al. (1988) pointed out that some geochemical characteristics of the ore are typical of volcanogenic, while others of hydrogenic Mn-deposits, with some of them having transitional values. As a conclusion, they suggested strong hydrothermal and limited hydrogenic contributions in the ore genesis. The diagenetic origin of rhodochrosite was proved by stable isotope data (Polgári et al., 1991). Polgári et al. (2000) suggest that the metals originated from a distant hydrothermal source, easily covered huge distances due to the special geochemical and circulation conditions in the World Ocean during the Toarcian, and that rhodochrosite formed during early diagenetic processes from the primarily precipitated manganese oxyhydroxides. Polgári (2001) gives an overview of the arguments that suggest fine-grained vitreous volcanic matter (glass, tuff) contribution to the basin sediments during the formation of the deposit. Lantos et al. (2003) implied that some fine particulate matter, originating from a hydrothermally altered basaltic sequence, rich in magnesium, manganese and iron, entered the suboxic local deep to form the base material of the ore mud. A significant amount of carbonate reached the deep from the adjacent slopes, and the present-day carbonate formed as a result of drastic early diagenetic transformation.

Fig. 3. Sample #URK6K (ID number of the bulk samples at the Natural History Museum of the Eötvös Loránd University: BE81854–BE81857): a banded manganese carbonate ore with the special green colour that is due to the high green phyllosilicate content. The 2 mm-thick pale yellow layer in the middle of the sample is a rhodochrosite layer, denoted as "whitish lamina" by Lantos et al. (2003). Parts of the sample BE81857, denoted as #U-1 (BE81858), #U-2 (BE81859) and #U-3 (BE81860) were used for preliminary control of the mineralogical homogeneity of the subsequent green bands.

Jenkyns et al. (1991), in their review of the Jurassic manganese carbonates of Central Europe, argued that the formation of an extended oxygen-minimum layer throughout the World Ocean can lead to a significant concentration of manganese (Mn^{2+}) in the ocean water, without any necessary volcanic source, however, they did not exclude the possibility of volcanic metal contribution in the case of ore grade manganese accumulations.

Sample preparation and separation control

Due to the mining operations going on for almost half a century now, a well-documented and carefully chosen set of manganese carbonate ore samples is at disposal. When selecting the proper sample for studying the green clay mineral, three major criteria were considered: (1) the 10-Å clay mineral should possibly be void of swelling components and the sample itself should not contain other layer silicates such as smectites or chlorites, as the separation of one layer silicate from another is practically impossible; (2) the 10-Å clay mineral should possibly be highly concentrated in the sample; (3) the amount of sample should be sufficient for purposes of separation and chemical analysis, all to be done on the very same sample. XPD data and colour information helped with finding the sample best meeting the requirements.

The availabe samples richest in celadonite, together with preliminary XPD data are listed in Table 1. The sample selected for further investigation (Fig. 3) originates from the top of the Main Ore Bed, at 283 m of Profile "B_3" of Shaft III (175 m above Baltic sea level), Western Mine Field, Úrkút (Fig. 1). It was collected by Polgári in 1989 (sample #URK/6) from a location that was sampled in the 1980s by

Table 1. Samples rich in the colouring green clay mineral, collected by Grasselly et al. ([1]: code used by Grasselly et al., [2]: code used by Polgári), their relation to the sample studied in this work ([3]: code used in the present work), and results of former (Polgári et al., 2000) X-ray powder diffraction studies ([4]) and preliminary X-ray powder diffraction studies done in this work ([5]). ([6]: Sample locality after Polgári et al. (2000), Vadász (1952) did not publish the exact locality of the sample. ≈: sample from the same occurrence, but not identical to the one collected formerly. ≡: identical sample. *: above Baltic sea level.)

Code[1]	Code[3]	Sample description	Sample locality	Stratigraphic position	Mineral composition[4] (Polgári et al., 2000)	Mineral composition[5] (this work)
#188		"Green clay" after Vadász		So-called "green clay" underlying the ore (Vadász, 1952)[6]		
#2		Dark grey radiolarian clay marl	Úrkút, Shaft III, Western Mine Field, Northern part (+256 m*), Profile "A"	Bed directly underlying the main ore bed	10-Å phyllosilicate, smectite (montmorillonite), glauconite, anatase, rutile, chlorite?, gypsum, dolomite, pyrite, quartz, feldspar?, zeolite (clinoptilolite, heulandite)	Main: quartz, smectite, Subordinate/trace: 10-Å phyllosilicate (001 strongly asymmetric), feldspar, pyrite, double carbonate (d_{104}=2.89 Å, e.g. dolomite), gypsum
#188a (≈#3a)		Green part of a green-grey carbonate ore sample	Úrkút, Shaft III, Western Mine Field, Northern part (+256 m*), Profile "A"	Lowermost layer of the main ore bed		Main: 10-Å phyllosilicate (001 symmetric, d_{060}=1.510 Å), quartz
#4a		Dark green part of a grey-green carbonate ore sample	Úrkút, Shaft III, Western Mine Field, Northern part (+256 m*), Profile "A"	Lower part of the main ore bed	Rhodochrosite, 10-Å phyllosilicate (glauconite), goethite, rutile	Main: 10-Å phyllosilicate (001 slightly asymmetric; d_{060}=1.510 Å), rhodochrosite, Subordinate/trace: goethite, quartz
#49	≈URK6K (≡URK/6,[2] collected by Polgári et al.) in July 1989	Green laminated carbonate ore	Úrkút, Shaft III, Western Mine Field, deep level (+175 m*), at 283 m of Profile "B_3"	Uppermost part of the main ore bed	Rhodochrosite, 10-Å phyllosilicate (celadonite), sericite, muscovite,goethite	Main: Rhodochrosite, 10-Å phyllosilicate (001 symmetric; d_{060}=1.510 Å), Subordinate/trace: goethite, quartz
#15		Radiolarian clay marl	Úrkút, Shaft III, Western Mine Field, Northern part (+256 m*), Profile "A"	Bed directly overlying the main ore bed	Quartz, pyrite, 10-Å phyllosilicate (illite, glauconite-celadonite), siderite, zeolite (clinoptilolite, heulandite?, mordenite), smectite (montmorillonite), dolomite, ankerite, rutile, gypsum, chlorite	Main: quartz, smectite, 10-Å phyllosilicate (001 asymmetric; d_{060} cannot be determined), Subordinate/trace: pyrite, zeolite (clinoptilolite/heulandite), double carbonates (d_{104}=2.98 Å; 2.87 Å)
#187		Average sample rich in celadonite	Úrkút	Collected at different points of the main ore bed		

Grasselly et al. (sample #49), too. For the complete documentation of these samples and former analyses performed on them see Polgári et al. (2000).

An amount of 186 g material was subjected to a three-step separation procedure (Fig. 4). Each separation step was documented by a few grams of reference material. XPD, FTIR spectroscopy and full chemical analysis were applied to monitor the course of the separation. For the complete documentation of the three-step separation procedure, together with the detailed description of the method developed for quartz removal from clay-sized materials see Weiszburg et al. (2004).

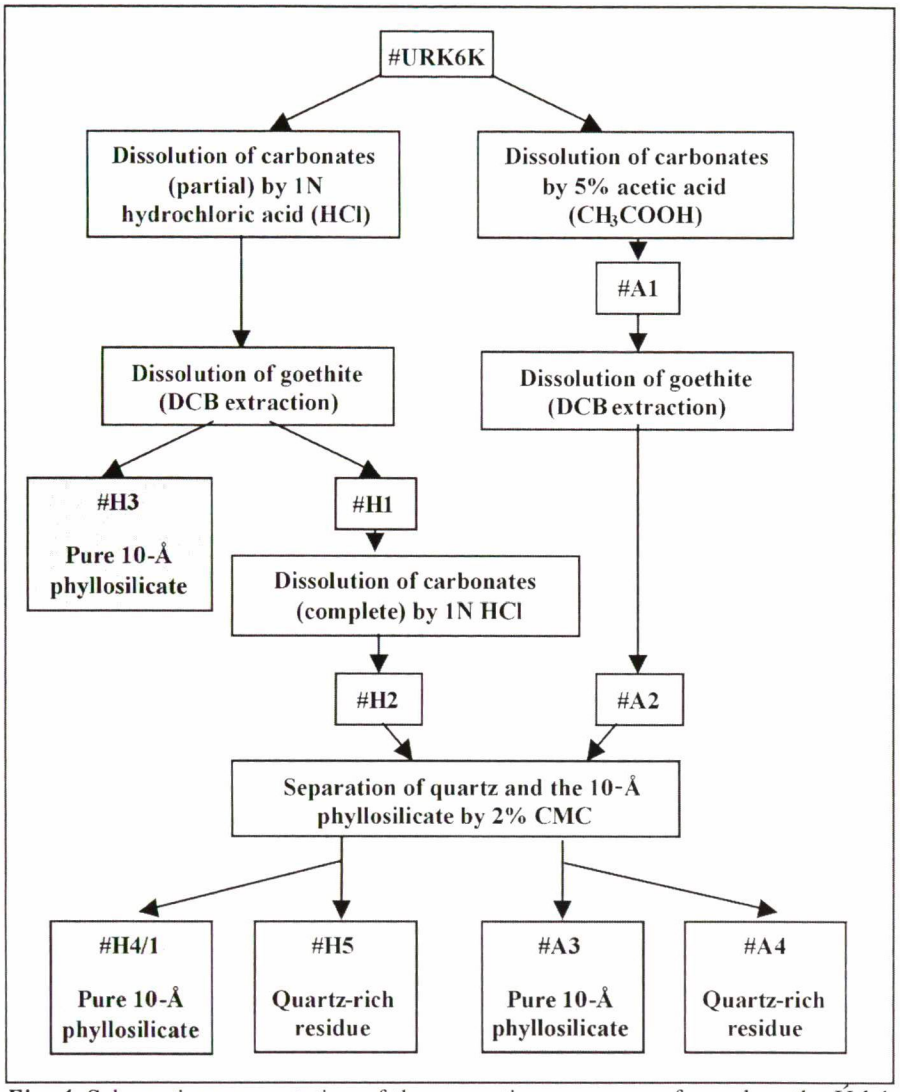

Fig. 4. Schematic representation of the separation process performed on the Úrkút manganese carbonate ore, sample #URK6K (BE81861: powdered reference sample). The starting material was 100 g in the case of the HCl separation branch and 50 g in the case of the acetic acid separation branch. Shaded boxes represent the pure samples subjected to detailed investigation. (BE81862: Reference samples on the hydrochloric separation branch; BE81863: Reference samples on the acetic acid separation branch; BE81864: Solution remaining after goethite removal on the acetic acid separation branch.)

Analytical methods

X-ray powder diffraction (XPD) patterns were obtained at the Department of Mineralogy, Eötvös Loránd University (Budapest). Most of the patterns were done on a SIEMENS D500 diffractometer of Bragg-Brentano geometry, equipped with secondary pyrolithic graphite monochromator and applying Cu-Kα radiation. Rotation speed of the goniometer was 2°/min. Patterns of the most interesting samples, including all the patterns published here, were obtained on a SIEMENS D5000 diffractometer of Bragg-Brentano geometry, equipped with secondary pyrolithic graphite monochromator and applying Cu-Kα radiation. Counting time was 10 seconds, step size was 0.05°. Oriented samples were prepared by applying drops of an ethanol-mica suspension on a glass slide, with the help of a pipette. For testing the quartz content of the pure samples, also precision patterns were obtained with detection time of 10 seconds and a step size of 0.02°.

Fourier transform infrared spectroscopy (FTIR) was done at the Institute of Mineralogy and Crystallography, University of Vienna. Powder spectra were recorded from 4000–400 cm^{-1} on a Perkin-Elmer FTIR spectrometer 1760 X equipped with a TGS detector, using a CsI microfocus accessory for the measurements of the prepared KBr micropellets. Background and sample spectra were obtained from 25 scans each with a nominal resolution of 2 cm^{-1}.

Transmission electron microscopy (TEM) was applied for the morphological observation of the green phyllosilicate. Images were obtained on a JEOL JEM 100U microscope at the Department of Mineralogy, Eötvös Loránd University. Selected area electron diffraction (SAED) patterns were obtained at 100 kV accelerating voltage and 120 mA beam current.

Bulk chemical analyses (inductively coupled plasma atomic emission spectrometry, ICP-AES) of the powdered samples were performed on a Jobin Yvon JY70 spectrometer at the Geological Institute of Hungary (MÁFI) by András Bartha and Éva Bertalan. The amount of FeO was determined by titration.

All samples (except for sample #URK6Kca) were fused with lithium metaborate before the analysis. The analysed samples weighed 1.24 g (#H4/1), 0.79 g (#H3) and 0.18 g (#A3). In the case of sample #URK6Kca concentrated acids (1 ml of cc HCl, HNO_3 and H_2F_2 each were added to 0.25 g of sample) were applied to decompose the silicate structures and in a second step 10 ml of saturated boric acid was added to the solution to bind excess fluoride.

Results

X-ray powder diffraction

XPD was used to (1) monitor the separation process, (2) test if the studied layer silicate contains any swelling component and (3) test the method that distinguishes between glauconite and celadonite upon the d_{060} value, as described by Buckley et al. (1978).

For shortage in pure phyllosilicate samples, oriented and oriented glycolated patterns (Fig. 5) were obtained on the samples still containing low amounts of quartz (sample #H2 and #A2, a few percentage). Neither asymmetric broadening on the lower 2θ-side of the 10 Å-reflection, nor reflection-shift on glycolation was observed. The d_{060} spacing of the studied phyllosilicate equals 1.510 Å (±0.001 Å).

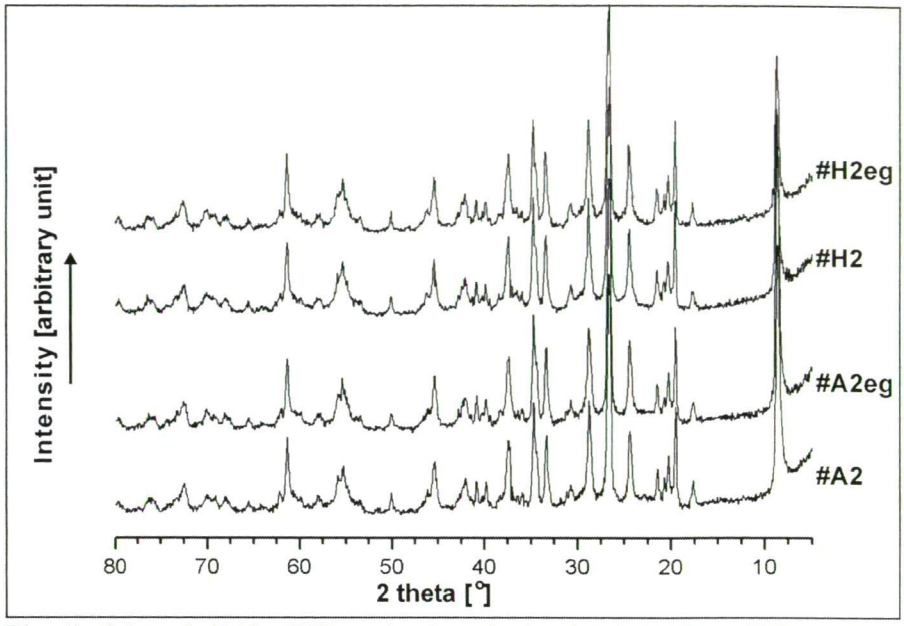

Fig. 5. Oriented (#A2, #H2) and oriented glycolated (#A2eg, #H2eg) X-ray powder diffraction patterns of the Úrkút green mica (Cu-Kα radiation)

Infrared spectroscopy

The FTIR spectra of the whole rock (sample #URK6K) and the separated phyllosilicate are presented in Fig. 6 and Table 2. Rhodochrosite is present in the whole rock as a major component (indicated by the strong absorption bands at around 1420, 866 and 726 cm^{-1}).

Goethite cannot be detected neither in the whole rock (≈8 wt%), nor in the pure samples (<1 wt%) as its main absorption bands (at 890 and 797 cm^{-1}, Farmer, 1974) are completely overlapping with intense celadonite absorption bands. The amount of goethite in the pure samples is smaller than 1%, the detection limit of voltammetry (Grygar et al., 2002), as measured by Grygar (personal communication, 2002).

Apatite has been indicated by small peaks and shoulders at around 603–605, 576 and 564–566 cm^{-1} (Farmer, 1974) in the whole rock (sample #URK6K) and in the pure sample #A3 (decarbonated by acetic acid) while it is missing from sample #H4/1 (decarbonated by HCl). These findings are in accordance with both the chemical data (phosphate contents are 0.23 and <0.02 wt% in samples #A3 and #H4/1, respectively) and the known acid resistance of apatite (it dissolves in HCl but not in acetic acid).

Quartz has a characteristic doublet at 798/780 cm^{-1}. This doublet is completely hidden by celadonite bands, however, there is a very weak shoulder at 780 cm^{-1} on each pattern. This shoulder might either refer to the small quartz impurities known from the XPD patterns or correspond to the shoulder visible at 777 cm^{-1} on the IR pattern of synthetic celadonites (both OH and OD varieties) of Russell et al. (1970).

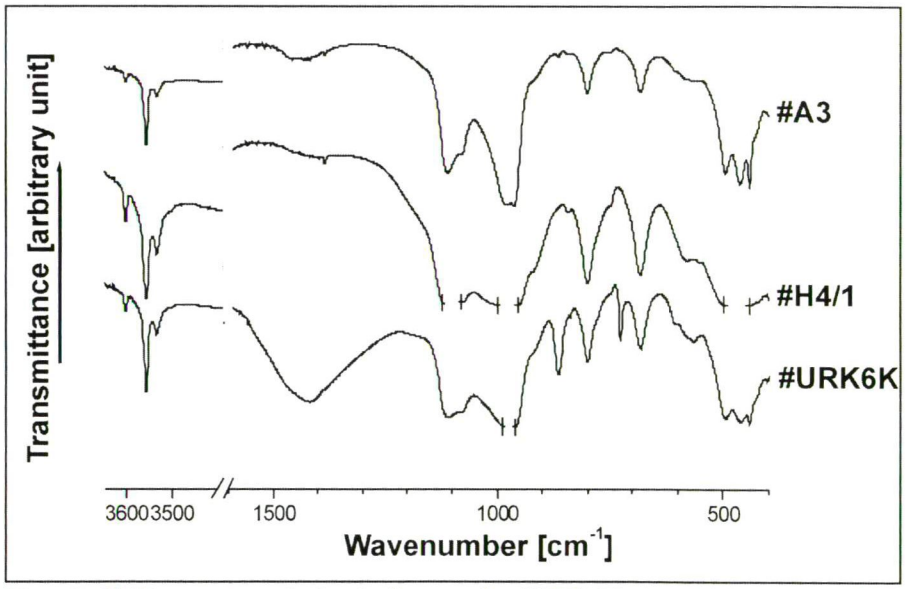

Fig. 6. FTIR spectra of the bulk sample #URK6K (containing appr. 40% rhodochrosite, as represented by absorption bands at around 1420, 866, 837 and 726 cm^{-1}; and smaller amounts of goethite, quartz and apatite, the latter being represented by small shoulders at around 606 and 576 cm^{-1}). Pure samples are #A3 (decarbonated by acetic acid and thus still containing traces of apatite, represented by small shoulders at around 606 and 576 cm^{-1}) and #H4/1 (decarbonated by hydrochloric acid and thus void of apatite). The sharp, distinct bands in the OH-stretching region (3700–3500 cm^{-1}) are typical of celadonite, as defined by Bailey (1980), based on Buckley et al. (1978). For comparison of the FTIR spectra of the Úrkút mica with those appointed to be typical of celadonite and glauconite see Fig. 7.

The clear and distinct absorption bands in the OH-stretching region indicate that the studied mineral has a well-ordered octahedral sheet.

TEM investigations

Samples #H3 and #H4/1 have been studied by transmission electron

Table 2. Band assignments of the FTIR spectra shown on Fig. 5.

identified phase					#URK6K			#H4/1			#A3		
name	assignment	w. n.	int.	prof.	w.n.	int.	prof.	w.n.	int.	prof.	w.n.	int.	prof.
C	ν Al-Mg-OH	3603	s l	shp	3602	s	shp	3602	s	shp	3602	s	shp
C	ν Al-Fe^{2+}-OH	3575-3577	s l	shp	3570	w	sh	3571	w	sh	3570	w	sh
C	ν Fe^{3+}-Mg-OH	3558	s	shp	3557	s	shp	3557	s	shp	3556	s	shp
C	ν Fe^{3+}-Fe^{3+}-OH ν Fe^{3+}-Fe^{2+}-OH	3535[1]	s	shp	3534	s	shp	3533	s	shp	3533	s	shp
R		1420	s	b	1419	s	b						
C	ν T (Si-O)	1110	s	shp	1109	s	b	n.d.			1108	s	shp
C	ν T (Si-O)	1070-1080	s	sh	1074	s	b	n.d.			1074	s	b
C[2]					n.d.			n.d.			980	s	b
C	ν T (Si-O)	955-970	s	b	n.d.			n.d.			961		
C[3]	δ Al-Al-OH	≈ 920	w	i	918	w	sh	918	w	sh	917	w	sh
R		866-867	s	shp	863	s	shp						
C	δ Al-Mg-OH	840	s l	shp				842	w	shp	841	w	b
R		837	w	sh	837	w	shp						
C	δ Fe^{3+}-Mg-OH δ Fe^{3+}-Fe^{2+}-OH	800	s	shp	800	s	shp	800	s	shp	800	s	shp
				sh	778	v w	sh	778	v w	i	781	v w	i
C	δ T (Al-O-Si)	748	w	b	746	w	sh	747	ss	sh	747	w	sh
R		726-727	s	shp	725	s	shp						
								686	v w	sh			
C[4]	δ Fe^{3+}-Mg-OH δ Fe^{3+}-Fe^{2+}-OH	679-680	s	shp	681	s	shp	681	s	shp	681	s	shp
A		603-605	s	shp	604	w	shp				606	w	sh
A		576	s	shp	579	v w	b sh	??579	w	sh	581	v w	b sh
A		564-566			564	w	shp				564	w	sh
C[2,4]		≈ 550	w	sh	551	v w	sh	552	w	sh	551	w	sh
C	δ T (Si-O)	488-492	s	shp	494	s	shp	n.d.			494	s	shp
C	δ T (Si-O)	460-462	s	b	460	s	b	n.d.			461	s	b
C	δ T (Si-O)	436-437	s	shp	440	s	shp	n.d.			440	s	shp
A		425		sh	425	w	sh	n.d.			426	w	sh

Legend: **C** - celadonite (peak positions and band assignments from Farmer (1974), Odin et al. (1988) and Beran (2002)); **R** - rhodochrosite (peak positions from Farmer (1974) and Jones and Jackson (1993)); **A** - apatite (peak positions of hydroxy- and fluorapatite from Farmer (1974)); **w.n.** - wave number (cm^{-1}); **n.d.** - no data due to non-transparency; **int.** - intensity; **s** - strong; **w** - weak; **v w** - very weak; **s l** - sometimes lacking; **prof.** -profile; **shp** - sharp; **b** - broad; **sh** - shoulder; **i** - inflection

[1]: Slonimskaya et al. (1986)

[2]: celadonite from Odin et al. (1988), as seen on Fig. 10 of page 355

[3]: a very weak shoulder at celadonite C44A in Odin et al. (1988), as seen on Fig. 10 of page 355. This band is assigned to δ Al-Al-OH in synthetic Mg-Al-celadonite by Velde (1978)

[4]: also present in synthetic Mg-Al-celadonite according to Velde (1978)

microscopy (TEM). The grains in both samples are euhedral laths (Fig. 8A), the only difference detected is the grain size. The length of the laths in sample #H4/1 is ranging between 2.09–0.09 μm, the width between 1.14–0.05 μm. Grain size distribution is more balanced in sample #H3, probably due to its separation mechanism (suspension, see above), with the grains falling in the lower size range of sample #H4/1: lath length is ranging between 0.9–0.09 μm and width between 0.45–0.06 μm.

The two samples were identical in their diffraction pattern, too. In the SAED pattern of sample #H4/1 (Fig. 8B) the lack of turbostratic structure (typical of illite-1Md and most glauconites) is also evident.

Chemical analysis

All separation steps were documented by full chemical analysis (for all the data and a detailed discussion see Weiszburg et al., 2004). Possible Li content of the green mica was checked (applying a different digestion method), but was found to be only in the trace element range (16–32 ppm). To check whether goethite has a significant manganese substitution (i.e. groutite component), as proposed by Lantos et al. (2003), the solution remaining after goethite removal (acetic acid separation branch) has also been analysed for Fe- and Mn-content.

Chemical formulae of the phyllosilicate were calculated from the

analyses of samples #A3, #H3 and #H4/1 (Tables 3-4). The chemical data of sample #A3 indicated the presence of some phosphate-bearing phase (P_2O_5 = 0.23 wt%), which has been confirmed by infrared spectroscopy, referring to apatite. The amount of CaO was thus reduced according to the P_2O_5-content in the analysis #A3 before the formula calculation.

Formulae of the green phyllosilicate were calculated for 11 O atoms. The total amount of Si was assigned to the tetrahedral position and Al was used to fill up the remaining tetrahedral sites. The rest of Al, together with Fe^{3+}, Fe^{2+}, Mg, Ti^{4+} and Mn^{2+} filled up the octahedral positions. Ti was assigned to the phyllosilicate as in case it was present in the form of rutile (or other TiO_2 polymorphs) in the ore, it should have got separated during the last separation step. K, Na and traces of Ca were assigned to the interlayer position. Loss of ignition was considered as water. After the deduction of the water amount required by the hydroxyl groups of the mica structure about one molecule water (p.f.u.) was still left. The calculated formulae are presented in Table 4.

A "residue" composition, denoted #R was also calculated using the chemical data of the untreated sample (#URK6K, after the subtraction of apatite and pyrite) and the data of the sample #H4/1. A linear equation system with 7 unknowns was set up: certain amounts of MnO, CaO, FeO, MgO (carbonate phase), Fe_2O_3 (goethite), SiO_2 (quartz) and derived ignition loss, corresponding to the CO_2-content of the carbonate phase and the H_2O-content of goethite, were subtracted from the chemical data of sample #URK6K to obtain the oxide values of the analysis #H4/1.

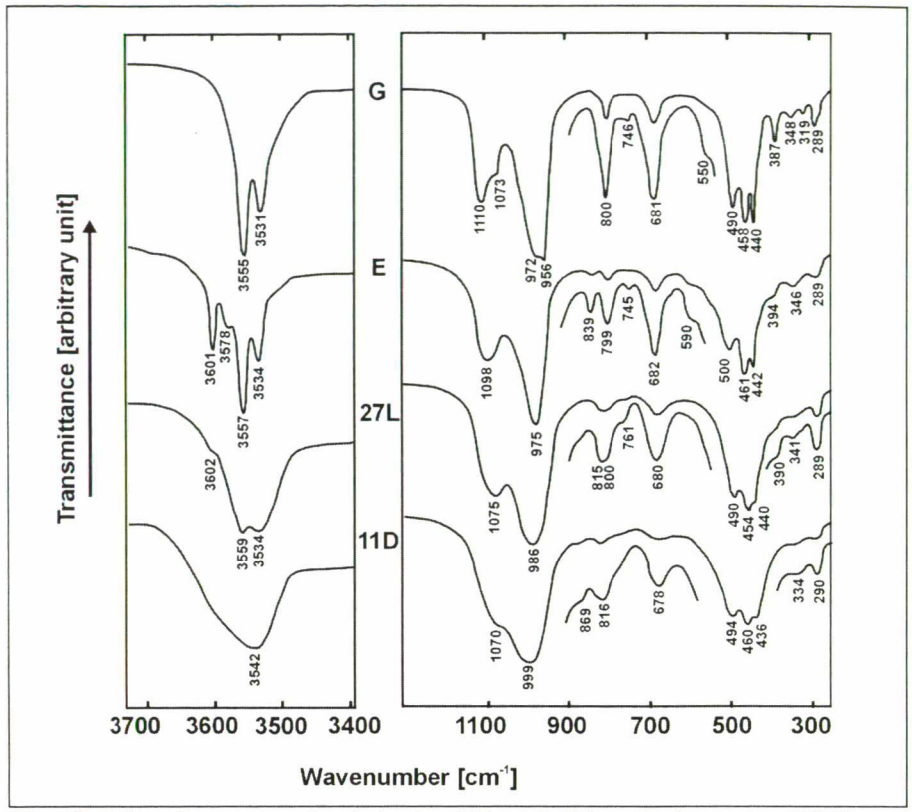

Fig. 7. Infrared patterns of celadonite (#G and #E) and glauconite (#27L and #11D) from Buckley et al. (1978). It is clear that the infrared spectra of the Úrkút green mica (Fig. 5.) are quite similar to the celadonite spectra in the OH-stretching region (3400–3700 cm^{-1}), and they differ significantly from the spectra published for glauconite.

The effect of quartz, a very small amount of which was indicated by XPD in the "pure" samples (except for sample #H3), on the formula of the phyllosilicate was also tested. For details see Weiszburg et al. (2004).

The above described consideration also allowed an estimation on the mineral composition of the studied ore sample (Table 5). Thus the composition of the ore richest in celadonite is the following: celadonite 43 wt%, carbonate 41 wt%, goethite 8 wt%, quartz 6 wt% and apatite 2 wt% (pyrite 0.23 wt%).

The mean composition of the carbonate phase(s?) is $MnCO_3$ 87 wt%, $CaCO_3$ 9 wt%, $MgCO_3$ 3 wt% and

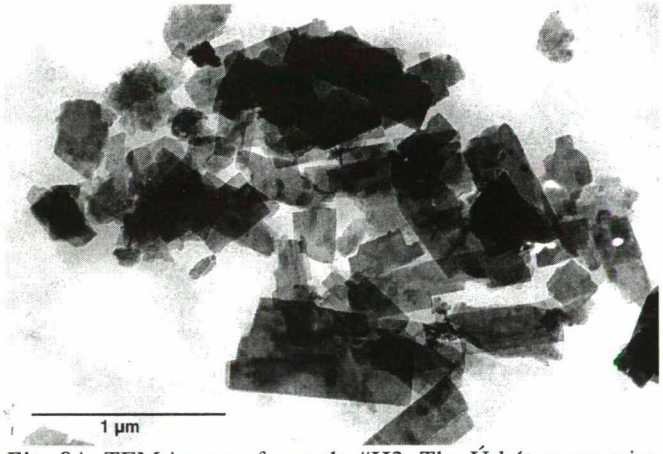

Fig. 8A. TEM image of sample #H3. The Úrkút green mica occurs as well-crystallised laths.

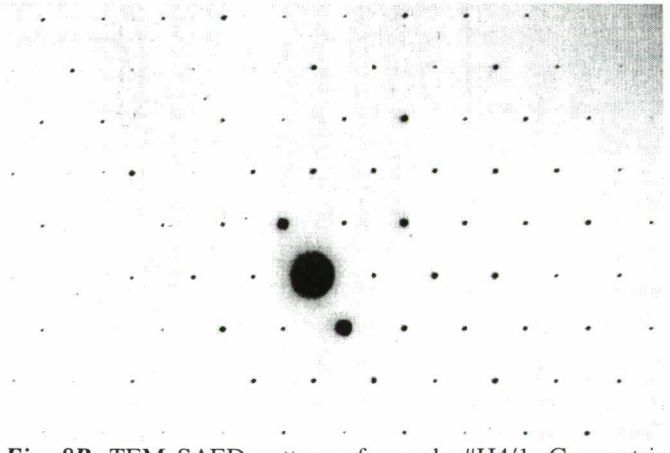

Fig. 8B. TEM SAED pattern of sample #H4/1. Concentric reflection circles (characteristic of illite-1Md and most glauconites) are missing.

$FeCO_3$ 1 wt%. XPD data of sample #URK6K shows the presence of only one cabonate phase (of calcite structure). Its most intensive $d_{(104)}$ reflection is at 2.86 Å. This value is slightly higher than that of pure rhodochrosite (2.84 Å), thus X-ray powder diffraction data do not contradict chemical data, indicating calcium substitution in rhodochrosite. FTIR data reveal only one carbonate phase, too.

Based on the analysis of the liquid remaining after goethite removal, Mn may substitute 5% of Fe in goethite (i.e. $(Fe_{0.95}Mn_{0.05})OOH$).

DISCUSSION

Chemical composition

Layer silicates are classified upon their chemical composition (Bailey, 1980, 1986; Rieder et al., 1998). Chemistry-based classification is especially emphasised in the 1980 AIPEA classification (Bailey, 1980) concerning glauconite and celadonite: "Mode of origin is not a criterion, and a green fecal pellet in a marine sediment that meets the definition for celadonite should be called celadonite".

The studied green phyllosilicate exhibits a clear dioctahedral character and has high interlayer cation content (Table 4). The interlayer cation is predominantly potassium, the octahedral position is dominated by trivalent iron and magnesium and the tetrahedral position has only minor aluminium content. Based on its chemical composition, it is classified as celadonite according to the three latest classification schemes (Bailey, 1980, 1986; Rieder et al., 1998; Table 6). To compare the chemical composition of the studied phyllosilicate with that of glauconite (series name for interlayer-deficient micas) and celadonite (true mica species), the compositional fields given by the nomenclatures have been transformed into a charge diagram (Fig. 9). This diagram has three axes (T, O, and IL) corresponding to the total cationic charges of the tetrahedral, octahedral and interlayer positions, respectively and can be considered as an intersection of the block diagram presented in Fig. 1. of Rieder et al. (1998) with an $^{VI}Al / (^{VI}Al + ^{VI}Fe^{3+})$ value in the 0–0.5 range. Our analytical data meet both the IMA (Rieder et al., 1998) and the AIPEA (Bailey, 1980, 1986) criteria (Fig. 9). Formerly published chemistry-based formulae (Table 7A, B) of this green mica, not considering possible impurities, plot outside both the glauconite and the celadonite fields (Fig. 10), thus emphasising the importance of minute separation or at least careful data processing (Table 7C).

Water content left after filling up of the mica formula is hard to interpret. Though in related layer silicates (glauconite, illite) more strongly bound water of about the here observed amounts is common (Földvári, M., personal communication, based on DTA/DTG data showing loss of water between 170–190 °C), in the present case neither the FTIR data, nor the calculation of the chemical formula (no – very few – empty interlayer positions available for water or H_3O^+) support the presence of such a high amount of water in the structure.

Table 3. Chemical analyses of sample #URK6K, #URK6Kca and the derived pure phyllosilicate samples #A3, #H3 and #H4/1. Analysts: Bartha, A. and Bertalan, É. (Geological Institute of Hungary). Data are given in weight percent, except for the lithium-content that is given in µg/g.

sample#	#URK6K	#URK6Kca	#A3	#H3	#H4/1
bulk rock	x	x			
separated from					
carbonates			x	x	x
goethite			x	x	x
quartz			x		x
SiO_2	29.7		53.6	52.9	53.9
TiO_2	0.08		0.06	0.07	0.09
Al_2O_3	1.51		2.18 [1]	2.53	2.84
Fe_2O_3 [2]	14.2		*15.9*	*18.7*	*16.2*
FeO [2]	1.4		*2.2*	*2.6*	*2.3*
MnO	21.30	21.26	0.40	0.33	0.28
CaO	2.97		0.63	0.06	0.06
MgO	3.41		6.44	7.26	6.46
Na_2O	0.07		0.07	0.10	0.22
K_2O	4.54		9.59	9.56	9.29
LOI	18.30		7.31	5.07	6.30
H_2O^-	0.40		0.00	0.84	1.18
P_2O_5	0.79		0.23	<0.02	<0.02
SO_3	0.30		0.09	<0.02	0.01
BaO	0.006		0.005	0.005	0.003
SrO	0.011		0.004	0.001	0.001
Σ	98.98		98.73	100.02	99.12
Fe_2O_3 (total)	15.7	15.68	18.4	21.6	18.7
Li [µg/g]	n.d.	16	n.d.	n.d.	n.d.
sample weight [g]	3.36 [3]		0.18	0.79	1.24

[1]: Low value, probably erroneous measurement. [2]: In the case of sample #URK6K, the amount of FeO has been determined by titration. Iron and manganese data obtained on differently digested portions of the same sample (#URK6K: lithium metaborate fusion and #URK6Kca: digestion with concentrated acids) are equal within the analytical error. In the case of samples #A3, #H3 and #H4/1, the total amount of iron was given only in the form of Fe_2O_3, and that value was divided according to $Fe^{2+} : Fe^{3+} = 14 : 86$, a ratio obtained on two independent samples (#H2 and #A2) that still contained quartz beside the green phyllosilicate (calculated values are shown in italics). [3]: total amount of sample subjected to the two digestion methods (#URK6K and #URK6Kca). n.d.: not determined.

FTIR and XPD data

Buckley et al. (1978), studying a great number of celadonites and glauconites, came to the conclusion that these minerals can be distinguished by both infrared spectroscopy and X-ray powder diffraction. The two analytical methods have been incorporated in the AIPEA nomenclature (Bailey, 1980) as tools proper for distinguishing between celadonite and glauconite. At the same

Table 4. Calculated formulae of the green clay mineral.

	A3	H3	H4/1	R
IL				
K	0.91	0.89	0.87	0.98
Na	0.01	0.02	0.03	0.02
Ca	0.03	0.00	0.01	0.00
Σ	0.95	0.91	0.91	1.00
Σcharge	0.98	0.91	0.92	1.00
O				
Fe^{3+}	0.89	1.03	0.90	0.91
Mg	0.72	0.79	0.71	0.72
Al	0.19	0.07	0.23	0.19
Fe^{2+}	0.14	0.16	0.14	0.14
Mn	0.03	0.02	0.01	0.02
Ti	0.00	0.00	0.00	0.01
Σ	1.97	2.07	1.99	1.99
ΣR^{2+}	0.89	0.97	0.86	0.88
ΣR^{3+}	1.08	1.10	1.13	1.10
Σcharge	5.02	5.24	5.11	5.10
T				
Si	4.00	3.85	3.97	3.90
Al	0.00	0.15	0.03	0.10
Fe^{3+}	0.00	0.00	0.00	0.00
Σ	4.00	4.00	4.00	4.00
Σcharge	16.00	15.85	15.97	15.90
O*	10.00	10.00	10.00	10.00
OH*	2.00	2.00	2.00	2.00
H_2O	1.64	0.47	1.10	0.38

IL: interlayer cation. O: cation in octahedral position. T: cation in tetrahedral position. *: fixed for the calculation.

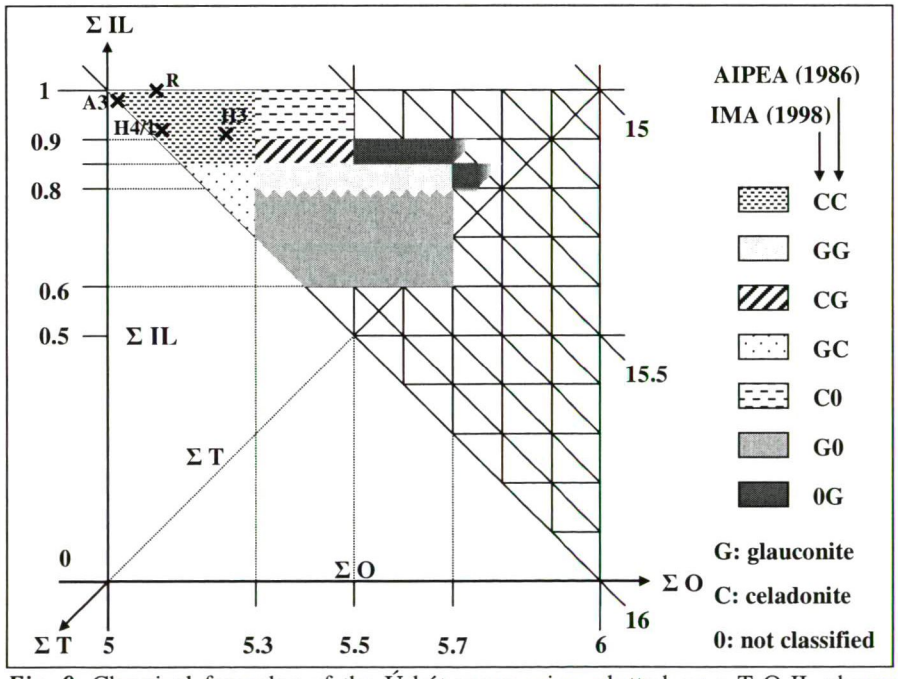

Fig. 9. Chemical formulae of the Úrkút green mica, plotted on a T-O-IL charge diagram. The horizontal axis (Σ O, values increasing right) of the diagram displays the total octahedral charge, the vertical axis (Σ IL, values increasing upwards) the total interlayer charge while the diagonal axis (Σ T, values increasing left downwards) the total tetrahedral charge. The total cation charge equals 22 at each point of the diagram. TOT layer silicates plot on the right half of the diagram (Σ T < 16, corresponding to max. 4 Si in the 4 tetrahedral positions). Our data plot in the CC field, thus the Úrkút green mica is classified as celadonite according to both the AIPEA (Bailey, 1980, 1986) and the IMA (Rieder et al., 1998) nomenclatures.

time they are not included (and can not be included) in the IMA nomenclature (Rieder at al., 1998), as it is obvious that part of Buckley's glauconites plot in the celadonite field of the IMA nomenclature (for a detailed discussion of the problem see Weiszburg et al., in prep).

FTIR

Our infrared spectroscopical data (Table 2, Fig. 6) agree well with the data published earlier for the Úrkút mineral by Kaeding et al. (1983), Pápay (1985) and Tóth (1990), and are quite similar to those published by Buckley et al. (1978) (Fig. 7) and others (e.g. Odin et al., 1988) for celadonite.

In the sense of the nomenclature of the AIPEA (Bailey, 1980), and based upon Buckley et al. (1978), infrared spectroscopy has been widely used as a reliable method for distinguishing between celadonite and glauconite. Both minerals have absorption bands at similar wavenumbers, but celadonite has sharp and distinct peaks in the OH-stretching region (3400–3700 cm^{-1}) while glauconite is characterised by less pronounced, broader peaks (Fig. 7). The sharpness of the absorption bands in the OH-stretching region is dependent on the cation ordering in the octahedral sheet. This is influenced by both the chemistry of the octahedral sheet and the tetrahedral Al substitution. The 1980 AIPEA nomenclature (Bailey, 1980) defines the border between the two minerals upon the tetrahedral Al substitution, the 1986 AIPEA nomenclature (Bailey, 1986) mainly upon the charge of the octahedral sheet, thus the AIPEA nomenclatures are somehow coherent

Table 5. Mineral composition of the studied ore sample and mean composition of the carbonate phase(s?).

Clay fraction	[weight%]
green clay mineral	43
Σ carbonate	41
goethite	8
quartz	6
hydroxylapatite	2
Σ	100
Carbonate phase(s?)	[weight%]
$MnCO_3$	87
$CaCO_3$	9
$MgCO_3$	3
$FeCO_3$	1
Σ	100

Table 6. Mineralogical definitions of celadonite and glauconite, based on the IMA and the AIPEA nomenclatures. The table also contains the corresponding parameters of the studied green clay mineral. All analyses fulfil the celadonite criteria of all three nomenclatures.

	CELADONITE	GLAUCONITE
IMA (Rieder et al., 1998)	$KFe^{3+}(Mg, Fe^{2+})\square Si_4O_{10}(OH)_2$ (mica end member *****) $^{VI}R^{2+} / (^{VI}R^{2+} + {}^{VI}R^{3+}) \geq 0.25$ $^{VI}Al / (^{VI}Al + {}^{VI}Fe^{3+}) < 0.5$ $Mg / (Mg + {}^{VI}Fe^{2+}) > 0.5$	$K_{0.8}R^{3+}_{1.33}R^{2+}_{0.67}\square Al_{0.13}Si_{3.87}O_{10}(OH)_2$ (series name) $^{VI}R^{2+} / (^{VI}R^{2+} + {}^{VI}R^{3+}) \geq 0.15$ $^{VI}Al / (^{VI}Al + {}^{VI}Fe^{3+}) \leq 0.5$
AIPEA (Bailey, 1980)	$KMgFe^{3+}Si_4O_{10}(OH)_2$ $^{IV}Al (^{IV}Fe^{3+}) = 0.0–0.2$ Σ IL charge > 0.6 *** $d_{060} < 1.510$ Å and sharp infrared spectra****	$K(R^{3+}_{1.33}R^{2+}_{0.67})(Si_{3.67}Al_{0.33})O_{10}(OH)_2$ $^{IV}Al (^{IV}Fe^{3+}) > 0.2$ * $^{VI}R^{3+} > 1.2$ * $Fe^{3+} >> Al$ ** $Mg > Fe^{2+}$ ** $d_{060} > 1.510$ Å and broader infrared spectra****
AIPEA (Bailey, 1986)	Σ O charge < 5.3	Σ O charge > 5.3; Σ IL charge = 0.8 – 0.9

	#H4/1	#A3	#H3	#R
$^{VI}R^{3+}$	1.13	1.08	1.10	1.10
$^{VI}R^{2+} / (^{VI}R^{2+} + {}^{VI}R^{3+})$	0.43	0.45	0.47	0.44
$^{VI}Al / (^{VI}Al + {}^{VI}Fe^{3+})$	0.20	0.18	0.06	0.17
$Mg / (Mg + {}^{VI}Fe^{2+})$	0.82	0.81	0.81	0.82
^{VI}Al	0.23	0.19	0.07	0.19
$^{VI}Fe^{3+}$	0.90	0.89	1.03	0.91
Mg	0.71	0.72	0.79	0.72
$^{VI}Fe^{2+}$	0.14	0.14	0.16	0.14
$^{IV}Al (^{IV}Fe^{3+})$	0.03	0.00	0.15	0.10
Σ IL charge	0.92	0.98	0.91	1.00
Σ O charge	5.11	5.02	5.24	5.10
Σ T charge	15.97	16.00	15.85	15.97

*Usually. **Unless altered. ***As defined by the upper limit for smectites. ****Further characteristics of the mineral, based on Buckley et al., 1978. *****In case of the IMA nomenclature, four end-members have been defined for celadonitic micas: celadonite, ferroceladonite, aluminoceladonite and ferro-aluminoceladonite. In the first two cases iron is the dominant trivalent octahedral cation, while in the others aluminium. Concerning divalent octahedral cations, magnesium dominates in celadonite and aluminoceladonite while iron dominates in ferroceladonite and ferro-aluminoceladonite. As the Úrkút green mica is inevitably celadonite, the criteria of only this mica have been plotted.

Table 7A. Formerly published analytical data of the Úrkút green mica.

Sample #			12	4758	4759		187	188	188a
Paper	Vadász (1952)[1]	Nagy (1955)[1]	Szabó-Drubina (1962)[2]	Kaeding et al. (1983)[3]	Kaeding et al. (1983)[3]	Dódony (1986)[3]	Polgári et al. (2000)[1]	Polgári et al. (2000)[1]	Polgári et al. (2000)[1]
Analyst	Grasselly		Jankovits				Bittó	Bittó	Bittó
SiO_2	65.34	54.25	50.51	56.10	55.70	-	47.54	47.60	63.72
TiO_2	0.21	-	0.53	0.10	0.10	-	0.26	0.10	0.21
Al_2O_3	5.00	5.95	4.15	2.60	3.60	-	2.97	3.95	1.78
Fe_2O_3	10.09	17.80	16.48	19.10	16.20	-	18.15	17.28	9.48
FeO	1.78	-	2.05	1.20	1.40	-	1.38	2.42	1.46
MnO	0.11	0.15	0.13	0.40	0.00	-	1.80	0.09	0.86
MgO	5.45	6.92	6.96	5.70	6.10	-	7.80	6.14	4.21
CaO	1.14	1.86	2.40	0.50	0.90	-	2.37	2.75	1.32
Na_2O	-	0.00	0.58	-	-	-	0.09	0.09	0.10
K_2O	5.61	8.40	7.72	7.70	10.10	-	8.45	8.37	4.92
MnO_2	-	-	-	-	n.d.	-	0.00	1.54	3.73
P_2O_5	0.40	-	1.09	0.2	0.30	-	1.35	1.69	0.14
LOI	-	5.30	-	-	-	-	-	-	-
H_2O^+	3.95	-	-	7.3	5.6	-	5.31	6.02	3.98
H_2O^-	1.85	-	-	-	-	-	1.58	1.14	0.64
CO_2	-	-	0.07	-	-	-	0.27	0.20	2.50
S	-	-	-	-	-	-	0.53	0.58	0.04
Total	100.93	100.63	92.67	100.90	100.00	-	99.85	99.96	99.09

[1]: For sample location see Table 1. [2]: Bluish green clay, Shaft I, sample #12 in Table 8 of Szabó-Drubina (1962). [3]: No data on the exact location of the sample.

Table 7B. Formulae calculated by the authors of the original papers.

Sample			#12	#4758	#4759		#187	#188	#188a
Paper	Vadász (1952)	Nagy (1955)	Szabó-Drubina (1962)	Kaeding et al. (1983)	Kaeding et al. (1983)	Dódony (1986)	Polgári et al. (2000)	Polgári et al. (2000)	Polgári et al. (2000)
Analyst	Grasselly		Jankovits				Bittó	Bittó	Bittó
Ref. to Fig. 10	1	2	3	4	5	6	7	8	9
IL									
K	-	-	-	0.70	0.92	0.725	0.826	0.844	0.44
Na	-	-	-	-	-	0	-	-	-
Ca	-	-	-	0.04	0.07	0	0.19	0.23	0.099
Σ	-	-	-	0.74	0.99	0.725	1.02	1.07	0.54
Σ charge	-	-	-	0.77	1.05	0.725	1.21	1.30	0.64
O									
Fe^{3+}	-	-	-	1.03	0.87	0	1.05	0.91	0.5
Al	-	-	-	0.25	0.29	1.275	0	0.13	0.15
Mg	-	-	-	0.61	0.65	0.725	0.89	0.72	0.44
Fe^{2+}	-	-	-	0.07	0.08	0	0.09	0.16	0.09
Σ	-	-	-	1.95	1.89	2.00	2.03	1.92	1.18
Σ charge	-	-	-	5.18	4.93	5.275	5.11	4.88	3.01
T									
Si	-	-	-	4.03	3.99	4	3.64	3.76	4.47
Al	-	-	-	-	0.01	0	0.27	0.24	0
O	-	-	-	10.00	10.00	10	10	10	10
OH	-	-	-	2.00	2.00	2	2	2	2
Σ	-	-	-	4.03	4.00	4.00	3.91	4.00	4.47
Σ charge	-	-	-	16.10	15.97	16.00	15.37	15.76	17.88
Σ cation charge	-	-	-	22.05	21.95	22.00	21.69	21.94	21.53

Table 7C. Recalculated formulae of the formerly published analytical data (Table 7A), after the subtraction of the 'impurities' indicated.

Sample			#12	#4758	#4759		#187	#188	#188a
Paper	Vadász (1952)	Nagy (1955)	Szabó-Drubina (1962)	Kaeding et al. (1983)	Kaeding et al. (1983)	Dódony (1986)	Polgári et al. (2000)	Polgári et al. (2000)	Polgári et al. (2000)
Analyst	Grasselly		Jankovits				Bittó	Bittó	Bittó
Ref. to Fig. 10	1	2	3	4	5	6	7	8	9
IL									
K	0.63	0.77	0.74	0.73	0.92	-	0.84	0.85	0.85
Na	0.00	0.00	0.08	0.00	0.00	-	0.01	0.01	0.03
Ca	0.06	0.00	0.08	0.02	0.04	-	0.05	0.03	0.00
Σ	0.69	0.77	0.90	0.75	0.96	-	0.90	0.89	0.88
Σ charge	0.74	0.77	0.98	0.77	1.00	-	0.95	0.92	0.88
O									
Fe^{3+}	0.67	0.82	0.93	1.07	0.87	-	1.06	1.03	0.97
Al	0.50	0.38	0.16	0.19	0.30	-	0.00	0.16	0.20
Mg	0.71	0.74	0.78	0.63	0.65	-	0.91	0.73	0.65
Fe^{2+}	0.13	0.13	0.13	0.07	0.08	-	0.05	0.12	0.16
Mn	0.01	0.01	0.00	0.00	0.00	-	0.09	0.00	0.00
Ti	0.01	0.00	0.03	0.01	0.01	-	0.02	0.00	0.02
Σ	2.04	2.08	2.04	2.00	1.91	-	2.12	2.05	2.00
Σ charge	5.27	5.36	5.22	5.27	5.01	-	5.33	5.30	5.21
T									
Si	3.98	3.88	3.80	3.96	3.99	-	3.71	3.79	3.91
Al	0.02	0.12	0.20	0.04	0.01	-	0.27	0.21	0.09
Fe^{3+}	0.00	0.00	0.00	0.00	0.00	-	0.01	0.00	0.00
Σ	4.00	4.00	4.00	4.00	4.00	-	4.00	4.00	4.00
Σ charge	15.98	15.88	15.80	15.96	15.99	-	15.71	15.79	15.91
Σ cat. charge	22.00	22.00	22.00	22.00	22.00	-	22.00	22.00	22.00
H_2O	0.30	0.19	-	1.62	0.67	-	0.72	1.13	1.60
Corrected by [wt%]									
hydroxylapatite	0.95	0.00	2.57	0.48	0.71	-	3.21	4.02	0.33
$CaCO_3$	0.00	3.32	0.00	0.00	0.00	-	0.00	0.33	2.02
$MgCO_3$	0.00	0.00	0.00	0.00	0.00	-	0.00	0.00	2.07
$MnCO_3$	0.00	0.00	0.18	0.00	0.00	-	0.71	0.15	1.39
quartz	20.00	0.00	0.00	3.00	0.00	-	0.00	0.00	35.00
pyrite	0.00	0.00	0.00	0.00	0.00	-	0.99	1.09	0.08

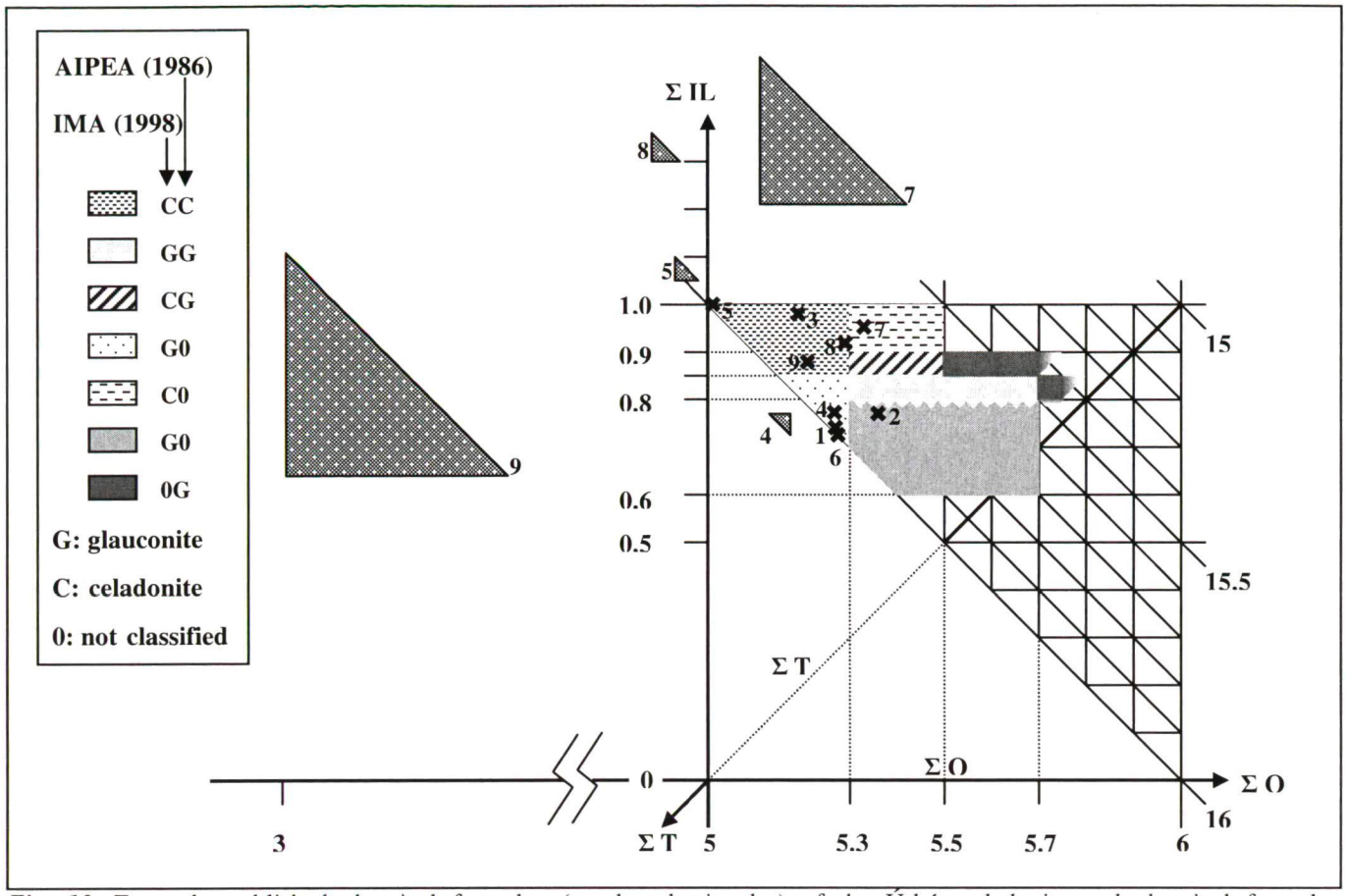

Fig. 10. Formerly published chemical formulae (numbered triangles) of the Úrkút celadonite and chemical formulae recalculated from the formerly published analytical data (numbered crosses), plotted on a T-O-IL charge diagram. Numbers refer to the publications: 1: Vadász (1952); 2: Nagy (1955); 3: Szabó-Drubina (1962); 4: Kaeding et al. (1983), sample #4758; 5: Kaeding et al. (1983), sample #4759; 6: Dódony (1986), based on crystallochemical calculations (1986); 7: Polgári et al. (2000), sample #187; 8: Polgári et al. (2000), sample #188; 9: Polgári et al. (2000), sample #188a.
Triangles of the formerly published formulae evolve from the fact that the total cationic charge of the mineral differs from 22 while the formula is calculated for 11 O atoms, i.e. –22 negative charge (The length of the perpendicular sides of the triangle equals the discrepancy between the total cationic charge and the theoretical value 22).
All formerly published formulae (except for that of Dódony, 1986) plot outside the charge field accepted for TOT layer silicates with monovalent interlayer cation (tetrahedral charge = 15–16, interlayer charge ≤ 1 and octahedral charge = 5–6). Sometimes really small corrections (e.g. subtraction of small amounts of apatite or carbonates according to the P_2O_5 and CO_2-contents, respectively) are sufficient to get formulae that are in accordance with the supposed TOT structure.
Concerning the corrected formulae, 5 (out of 8) formulae (No. 3, 5, 7, 8 and 9) plot in the celadonite compositional field of the IMA nomenclature (Rieder et al, 1988), while 7 (No. 1, 2, 3, 4, 5, 6 and 9) and another 7 (1, 3, 4, 5, 6, 8 and 9) formulae plot in the celadonite field of the two AIPEA nomenclatures (Bailey, 1980, 1986). 3 formulae (3, 5 and 9) are classified as celadonite in all three nomenclatures.

with the infrared spectroscopical data of the literature (e.g. Buckley et al., 1978; Odin, 1988). The IMA nomenclature (Rieder et al., 1998), on the other side, differentiates between the two minerals upon the interlayer content, suggesting that celadonites and glauconites can have similar tetrahedral Al substitution, similar $^{VI}R^{2+}$ / $^{VI}R^{3+}$ ratio and consequently, similar grade of ordering in the octahedral sheet and similar infrared pattern shapes. These different approaches may lead to confusion in the case of (1) Fe^{3+}-rich dioctahedral micas on the far right side of the celadonite field of the IMA nomenclature (see Fig. 9 and Fig. 10), i.e. celadonites with significant tetrahedral Al-substitution and $^{VI}R^{2+}$ / $^{VI}R^{3+}$ ratio considerably smaller than 1; (2) Fe^{3+}-rich dioctahedral micas on the left side of the glauconite field of the IMA nomenclature, i.e. glauconites with small or no tetrahedral Al-substitution. Fortunately, the studied green clay from Úrkút does not plot in these problematic regions of the diagram, so in this case Buckley's IR criteria can be applied.

XPD

The symmetric, for glycolation not responding 001 XPD reflections suggest the absence of swelling component in mica.

Our measurement gave the d_{060} spacing of the Úrkút green phyllosilicate to be 1.510 ± 0.001 Å. These values are close to, but slightly higher than the data formerly given on this mineral (Tóth, 1985, 1990; d_{060} between 1.507–1.509 Å).

Buckley et al. (1978) supposed an almost linear relationship between the octahedral Fe^{3+}-content of the

phyllosilicate and the d_{060} spacing, and suggested that the phyllosilicate is celadonite if the $d_{060} < 1.51$ Å and glauconite if $d_{060} > 1.51$ Å. The 1.510 Å d_{060} value was given as a discriminating value by the AIPEA nomenclature (Bailey, 1980).

The IMA nomenclature (Rieder et al., 1998) does not deal with the applicability of any simple and practical XPD parameter for that discrimination, moreover, it is clear that the IL occupancy should not be in direct relationship with the d_{060} spacing in the mica structure.

Fig. 11 shows that the d_{060} value of the Úrkút green mica plots right into the empty celadonite-glauconite border zone of Buckley et al. (1978). This observation suggests that there are cases when X-ray powder diffraction data can not be used so clearly for the discrimination between celadonite and glauconite, even in the AIPEA nomenclature system.

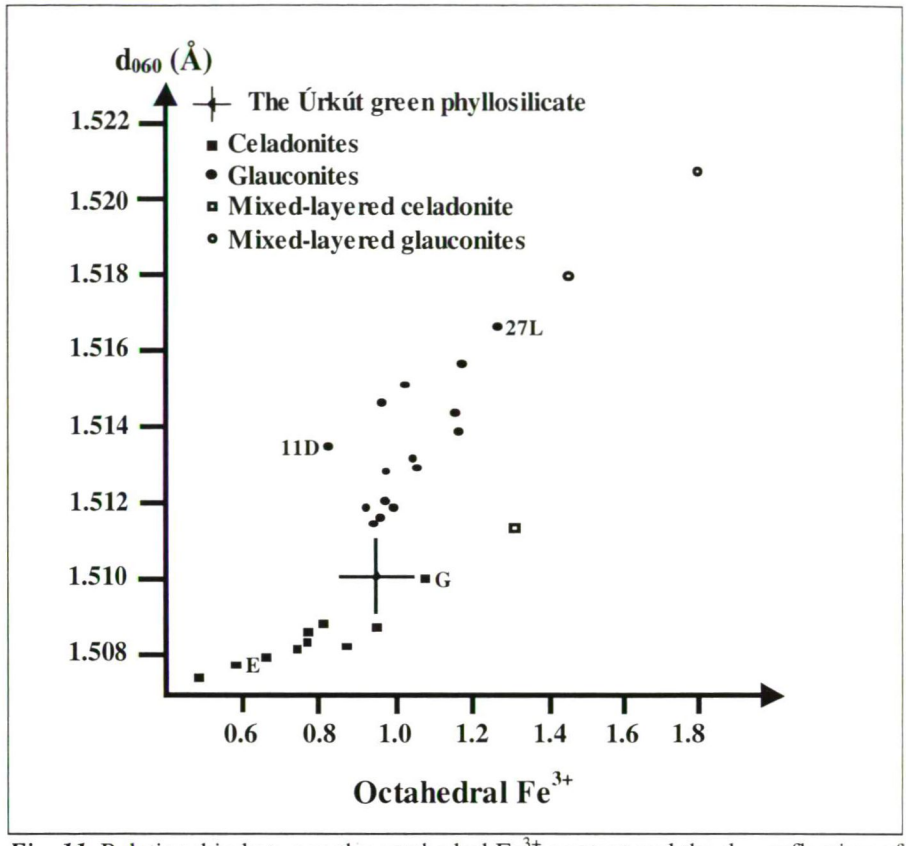

Fig. 11. Relationship between the octahedral Fe^{3+}-content and the d_{060} reflection of celadonites and glauconites, as presented by Buckley et al. (1978). #E and #G are celadonites while #11D and #27L are glauconites (their IR spectra are shown on Fig. 7). Data of the Úrkút green phyllosilicate are shown with error bar. Together with sample #G of Buckley et al. (1978), the infrared spectra of which was presented as typical for celadonite, the Úrkút green phyllosilicate plots exactly on the celadonite-glauconite border, as defined by Buckley et al. (1978) and incorporated in the AIPEA nomenclature by Bailey (1980).

Aspects of genesis

The findings from TEM investigations, namely that the mineral is predominantly an 1M polytype (Dódony, 1986), occurs as euhedral laths, exhibits no signs of turbostratic structure, together with the lack of swelling components and the high interlayer-content suggest that the studied mineral is a well-crystallised true mica formed by primary precipitation.

Our results contradict the opinion of Varentsov et al. (1988), who explained the formation of the "1M celadonite-type Fe-mica" by transformation from Fe-smectites during early diagenetic processes.

A problem is rising, however, from this mica being celadonite: the lack of volcanic rocks is a strong discrepancy between the Úrkút occurence and the known occurrences of celadonite-CC (celadonite in the sense of CC in Fig. 9 and Fig. 10; for further details see Weiszburg et al., in prep.). Celadonite-CC has only been observed in intimate association with basic volcanic rocks so far (Buckley et al., 1978; Odom, 1984; Odin et al., 1988). It has been described from oceanic basalts as (1) vesicle fillings (vesicle diameter 0.1–15 mm); (2) replacement of phenocrysts like olivine, pyroxene and plagioclase and even the groundmass of volcanic rocks; (3) diffuse celadonite in tuffs and altered lava flows; (4) films e.g. around voids filled with zeolites and calcite; (5) veins, fissures and lenses filled by celadonite–CC, with veins and fissures sometimes even having a thickness of tens of centimeters (Odin et al., 1988). Odin et al. (1988) suggest that celadonite is a synsedimentary–early diagenetic mineral that is formed from low-temperature interstitial waters of marine origin that became enriched in ions while circulating through a basaltic rockpile. From oxygen isotopic data the formation temperature of celadonite–CC is estimated to range between 50 °C and the temperature of seawater. Basic rocks are thus supposed to play an important role in celadonite genesis both as the source of cations and the host rock or substrate of the mineral.

The Úrkút manganese ore, in contrast, was formed in a sedimentary environment and no Toarcian volcanic rocks have been reported from the area. Celadonite–CC occurs as a constituent of the clay-sized ore material and its proportion varies widely in the ore bands. Kaeding et al. (1983), considering the absence of altered eruptive rocks, assumed that celadonite could have precipitated from hydrothermally modified sea- or porewater in a way similar to the accompanying montmorillonites i.e. by adsorption of silica onto the surface of iron oxyhydroxides and mixed Fe-Al gels. In their interpretation, seawater becomes rich in CO_2 due to volcanism and is thus able to mobilise and transport elements far away from the source volcanic rocks. In the model of Kaeding et al. (1983), the rocks that form the ion-rich solutions and the minerals that precipitate from these solutions are spatially separated; the model solves the problem of the lack of volcanic rocks and is otherwise close

to the genetic picture outlined by Odin et al. (1988) for celadonite. Similar approach has been adapted for the problem of lack of volcanic rocks by Polgári et al. (2000), while Lantos et al. (2003) implies that fine particulate matter (remnants of a basaltic sequence) was transported into the anoxic deep to form the base material of the ore.

Manganese-bearing Toarcian black shales are widespread in the Alpine Europe and represent the world-wide significant Toarcian Oceanic Anoxic Event (Jenkyns, 1988; Jenkyns et al., 1991). As pointed out by Jenkyns et al. (1991), the formation of an extended oxygen minimum layer can lead to a significant enrichment of manganese in the sea water and thus it is not necessary to assume a volcanogenic source of this metal in these shales, though it might be supposed at ore grade enrichment. According to the authors of the present paper, it is exactly the presence of well-ordered 1M polytype celadonite (together with the unique enrichment of manganese among the Toarcian Mn-bearing black shales of Europe) that suggests volcanogenic contribution to the genesis of the Úrkút manganese ore.

The present genetic interpretation of the Úrkút celadonite, as a precipitate syngenetic with the embedding ore, would indicate a Toarcian age for that mineral. The only radiometric data available, 151±6 and 166±7 Ma (Grasselly et al., 1994), show clearly younger ages by about 20–30 Ma. A similar situation was observed by Odin et al. (1988) for celadonite in a Toarcian basaltic sequence in Teruel, Spain, where the apparent age of celadonite was 147.7±3.0 (Rb-Sr) and 153±6 (K-Ar) Ma. When explaining the age misfit in the basaltic complex of Teruel, Odin et al. (1988) had to calculate with both real (postgenetic alteration of the basalt) and artificial (Ar release) causes. The undisturbed sedimentary record in Úrkút, embedding celadonite, without known primary volcanic rocks, reduces very much the space for a postgenetic effects-based interpretation of the younger age. A more detailed discussion of the age issues will be published elsewhere.

It is important to note that green peloids and elongated, platy green grains much resembling to glauconite grains have also been reported from the manganese carbonate ore under the term glauconite (Szabó-Drubina, 1957, 1959, 1962). Polgári et al. (2003) pointed out that these grains were originally not studied by any relevant analytical technique, thus they can be called only glaucony. Pekker et al. (2003), studying the insoluble fraction of the limestone formation overlying the manganese ore in Úrkút found green rounded grains, resembling somewhat to glauconite grains. These grains could not be determined properly, but their chemical composition (based on SEM+EDX measurements) excludes the celadonite-glauconite series and suggests them to be a mixture of iron-oxides(s) and some kind of oxidised chlorite, or chemically related substance. As a closing of the "glauconite-issue" in Úrkút, we can state, that for the moment there is not a single proved observation that would indicate the presence of a second type of green mica in Úrkút beside celadonite.

Conclusions

By studying a pure separate of the 10-Å phyllosilicate of the Toarcian Úrkút manganese carbonate ore, obtained by a three-step separation procedure, it has been unambiguously proved that the dominant, colour-giving green clay mineral of the ore is not glauconite, but well-crystallised celadonite (celadonite-CC, Weiszburg et al. in prep), that was formed by primary precipitation.

Though the Úrkút occurrence differs from the known celadonite occurrences in that it is not found in direct association with submarine basic volcanic rocks, the authors of this paper consider its presence in the ore as an evidence for volcanic contribution to the ore genesis.

Based on X-ray powder diffraction data of the Úrkút celadonite, doubts have been risen concerning the general applicability of the d_{060} spacing as a distinguishing feature between glauconite and celadonite (in the sense of AIPEA; Bailey, 1980) and thus review of the method suggested by Buckley et al. (1978) and accepted by Bailey (1980) is proposed.

Acknowledgements

The authors express their gratitude to Márta Polgári for providing the samples and making available all the information compiled formerly on the ore. Zoltán Szabó is thanked for his helpful guidance through the mine. The authors are grateful to András Bartha, Éva Bertalan and Tomáš Grygar for their kind help in the preparation of the analytical data and József Mizák, Tibor Nagy and Zsuzsanna Varga for the sample preparation.

The two reviewers, István Vető and István Viczián, as well as István Dódony, Zoltán Lantos and György Lovas are thanked for their kind help and useful comments concerning the manuscript.

This work was supported by OTKA (Hungarian National Science Foundation) Grant #T25873.

References

Bailey, S. W. (1980): Summary of recommendations of AIPEA Nomenclature Committee. Clays and Clay Minerals, **28**, 73–78.

Bailey, S. W. (1986): Report of AIPEA Nomenclature Committee. Supplement to AIPEA Newsletter No. 22.

B. Árgyelán, G., Császár, G. (1998): Detrital chrome spinels in Jurassic formations of the Gerecse Mountains, Hungary (*in Hungarian*). Földtani Közlöny, **128**, 321–360.

Beran, A. (2002): Infrared spectroscopy of micas. In Mottana, A., Sassi, F. P., Thomson Jr., J. B., Guggenheim, S. (eds): Micas: Crystal Chemistry and Metamorphic Petrology, Reviews in Mineralogy and Geochemistry, **46**, Mineralogical Society of America, Washington D. C. and Accademia Nazionale dei Lincei, Roma, 351–369.

Buckley, H. A., Bevan, J. C., Brown, K. M., Johnson, L. R., Farmer, V. C. (1978): Glauconite and celadonite: two separate mineral species. Mineralogical Magazine, **42**, 373–382.

Dódony, I. (1986): Electronmicroscopical study of the microstructure of fine-grained rocks. Textural and mineralogical study of the Úrkút glauconite-bearing manganese ore (*in Hungarian*). Research report, Department of Mineralogy, Eötvös Loránd University, Budapest, 19 p. (Referred in details in Polgári et al., 2000.)

Farmer, V. C. (ed.) (1974): The infrared spectra of minerals. Mineralogical Society Monograph 4, Mineralogical Society, London, 539 p.

Grasselly, Gy., Polgári, M., Tóth, M., Pápay, L., Filep-Molnár, E., Geiger, J. (1985): Complex geochemical, mineralogical and petrological study of the genetic and economic aspects of Hungarian manganese ore deposits (*in Hungarian*). Research report, Archive of the Hungarian Geological Survey, 583 p. (Referred in details in Polgári et al., 2000.)

GRASSELLY, GY., PANTÓ, GY., SZABÓ, Z. (1990): Mineralogical, geochemical and genetic study of Hungarian manganese ores (*in Hungarian*). Research report, Archive of the Hungarian Geological Survey, 277 p. (Referred in details in Polgári et al., 2000.)

GRASSELLY, GY., BALOGH, K., TÓTH, M., POLGÁRI, M. (1994): K/Ar age of manganese oxide ores of Úrkút, Hungary: Ar retention in K-bearing Mn minerals. Geologica Carpathica, **45/6**, 365–373.

GRYGAR, T., DĚDEČEK, J., HRADIL, D. (2002): Analysis of low concentration of free ferric oxides in clays by VIS diffuse reflectance spectroscopy and voltammetry. Geologica Carpathica, **53**, 71–77.

JENKYNS, H. C. (1988): The Early Toarcian (Jurassic) Anoxic Event: stratigraphic, sedimentary and geochemical evidence. American Journal of Science, **288**, 101–151.

JENKYNS, H. C., GÉCZY, B., MARSHALL, J. D. (1991): Jurassic manganese carbonates of Central Europe and the Toarcian Anoxic Event. Journal of Geology, **99**, 137–149.

JONES, G. C., JACKSON, B. (1993): Infrared transmission spectra of carbonate minerals. Chapman & Hall, London, 256 p.

KAEDING, L., BROCKAMP, O., HARDER, H. (1983): Submarin-hydrothermale Entstehung der sedimentären Mangan Lagerstätte Úrkút/Ungarn (*with English abstract*). Chemical Geology, **40**, 251–268.

LANTOS, Z., VETŐ, I., FÖLDVÁRI, M., KOVÁCS-PÁLFFY, P. (2003): On the role of remote magmatic source and intrabasinal redeposition in the genesis of the Toarcian Úrkút Manganese Ore, Hungary. Acta Geologica Hungarica, **46/4**, 321–340.

MIZÁK, J., VARGA, ZS., WEISZBURG, T. G., NAGY, T., LOVAS, GY. A., BARTHA, A., BERTALAN, É. (2000): Separation of the 10-Å green clay mineral from the carbonatic manganese ore, Úrkút, Hungary. Minerals of the Carpathians Conference, Miskolc, Acta Mineralogica-Petrographica, **41**, Suppl., 73.

NAGY, K. (1955): Mineralogical characteristics of the Úrkút carbonate manganese ore. (*in Hungarian with English and Russian abstracts*). Földtani Közlöny, **85**, 145–152.

ODIN, G. S., DESPRAIRIES, A., FULLAGAR, P. D., BELLON, H., DECARREAU, A., FRÖHLICH, F., ZELVEDER, M. (1988): The celadonite-bearing facies. In Odin, G. S. (ed.): Green marine clays. Developments in Sedimentology, **45**. Elsevier, Amsterdam, 333–398.

ODOM, I. E. (1984): Glauconite and celadonite minerals. In Bailey, S. W. (ed.): Micas, Reviews in Mineralogy, **13**, Mineralogical Society of America, Washington D. C., 545–572.

PÁPAY, L. (1985): Infrared spectroscopical data of the samples of the manganese carbonate gallery profile, Shaft III, Úrkút (*in Hungarian*), 98-115. In: Grasselly, Gy., Polgári, M., Tóth, M., Pápay, L., Filep-Molnár, E., Geiger, J.: Complex geochemical, mineralogical and petrological study of the genetic and economic aspects of Hungarian manganese ore deposits (*in Hungarian*). Research report, Archive of the Hungarian Geological Survey, 583 p. (Referred in details in Polgári et al., 2000.)

PEKKER, P., WEISZBURG, T. G., POLGÁRI, M. (2003): Micromineralogical and clay mineralogical study of the Eplény Limestone Formation, Úrkút, Hungary. Acta Mineralogica-Petrographica, Abstract Series, **1**, 85.

POLGÁRI, M. (2001): Contribution of volcanic material? A new aspect of the genesis of the black shale-hosted Jurassic Mn-carbonate ore formation, Úrkút Basin, Hungary. Acta Geologica Hungarica, **44/4**, 419–438.

POLGÁRI, M., OKITA, P. M., HEIN, J. R. (1991): Stable isotope evidence for the origin of the Úrkút manganese ore deposit, Hungary. Journal of Sedimentary Petrology, **61**, 384–393.

POLGÁRI, M., SZABÓ, Z., SZEDERKÉNYI, T. (2000): Manganese ores in Hungary (*in Hungarian with English summary*). Regional Committee of the Hungarian Academy of Sciences, Szeged, 652 p.

POLGÁRI, M. SZABÓ-DRUBINA, M., HEIN, J. R., SZABÓ, Z. (2003): Mn carbonate from the Eplény Mine, Hungary and chemical, mineralogical and stable isotope comparisons with other Jurassic Mn-carbonate deposits: Analyses of archive sample, No I. Földtani Közlöny, **133**/1, 21–35.

RIEDER, M., CAVAZZINI, G., D'YAKONOV, Y. S., FRANK-KAMENETSKII, V. A., GOTTARDI, G., GUGGENHEIM, S., KOVAL, P. V., MÜLLER, G., NEIVA, A. M. R., RADOSLOVICH, E. W., ROBERT, J. L., SASSI, F. P., TAKEDA, H., WEISS, Z., WONES, D. R. (1998): Nomenclature of the micas. The Canadian Mineralogist, **36**, 905–912.

RUSSELL, J. D., FARMER, V. C., VELDE, B. (1970): Replacement of OH by OD in layer silicates, and identification of the vibrations of these groups in infra-red spectra. Mineralogical Magazine, **37**, 869–879.

SLONIMSKAYA, M. V., BESSON, G., DAINYAK, L. G., TCHOUBAR, C., DRITS, V. A. (1986): Interpretation of the IR spectra of celadonites and glauconites in the region of OH-stretching frequencies. Clay Minerals, **21**, 377–388.

SZABÓ, Z., GRASSELLY, GY., CSEH NÉMET, J. (1981): Some conceptual questions regarding the origin of manganese in the Úrkút deposit, Hungary. Chemical Geology, **34**, 19–29.

SZABÓ-DRUBINA, M. (1957): Geological and mineralogical features of the Hungarian manganese ores (*in Hungarian with French abstract*). Földtani Közlöny, **87**, 261–273.

SZABÓ-DRUBINA, M. (1959): Manganese deposits of Hungary. Economic Geology, **54**, 1078–1093 (*extended version of Szabó-Drubina, 1957*).

SZABÓ-DRUBINA, M. (1961): Liassic manganese ore deposits of the Bakony Mountains. MÁFI Évkönyv, **49/4**, 951–957. (*in Hungarian*)

SZABÓ-DRUBINA, M. (1962): Petrological study of the Jurassic formations of the Bakony Mountains (*in Hungarian with French and Russian abstracts*). Annual Report of the State Geological Institute of Hungary on the Year 1959, 99–151.

TÓTH, M. (1985): X-ray powder diffraction data of the samples of the manganese carbonate gallery profile, Shaft III, Úrkút (*in Hungarian*), 115-150. In: Grasselly, Gy., Polgári, M., Tóth, M., Pápay, L., Filep-Molnár, E., Geiger, J.: Complex geochemical, mineralogical and petrological study of the genetic and economic aspects of Hungarian manganese ore deposits (*in Hungarian*). Research report, Archive of the Hungarian Geological Survey, 583 p. (Referred in details in Polgári et al., 2000.)

TÓTH, M. (1990): The question of the Úrkút celadonite (*in Hungarian*), 184-207. In: Grasselly, Gy., Pantó, Gy., Szabó, Z. (1990): Mineralogical, geochemical and genetic study of Hungarian manganese ores (*in Hungarian*). Research report, Archive of the Hungarian Geological Survey, 277 p. (Referred in details in Polgári et al., 2000.)

VADÁSZ, E. (1952): Manganese accumulation in the Bakony Mountains (*in Hungarian*). MTA Műszaki Osztály Közleményei, **5**, 231-261.

VARENTSOV, I. M., GRASSELLY, GY., SZABÓ, Z. (1988): Ore formation in the early-Jurassic basin of Central Europe: Aspects of mineralogy, geochemistry and genesis of the Úrkút manganese deposit, Hungary (*with German abstract*). Chemie der Erde, **48**, 257–304.

VELDE, B. (1978): Infrared spectra of synthetic micas in the series muscovite-MgAl celadonite. American Mineralogist, **63**, 343–349.

VÖRÖS, A. (1986): Brachiopod palaeoecology on a Tethyan Jurassic seamount (Pliensbachian, Bakony Mountains, Hungary). Palaeogeography, Palaeoclimatology, Palaeoecology, **57**, 241–271.

VÖRÖS, A., GALÁCZ, A. (1998): Jurassic palaeogeography of the Transdanubian Central Range (Hungary). Rivista Italiana di Paleontologia e Stratigrafia, **104**, 69–84.

WEISZBURG, T. G., NAGY, T., TÓTH, E., MIZÁK, J., VARGA, ZS., LOVAS, GY. A., VÁCZI, T. (2004): A laboratory procedure for separating micas from quartz in clay-sized materials. Acta Mineralogica-Petrographica, **45/1**, 133–139.

WEISZBURG, T. G., TÓTH, E., POP, D. (in prep): Comparison of the currently used nomenclatures of the celadonite-glauconite minerals.